

# Supplemental Material: Orbital-selective Mott phase and non-Fermi liquid in FePS<sub>3</sub>

Minsung Kim,<sup>1</sup> Heung-Sik Kim,<sup>2</sup> Kristjan Haule,<sup>1</sup> and David Vanderbilt<sup>1</sup>

<sup>1</sup>*Department of Physics and Astronomy, Rutgers University, Piscataway, New Jersey 08854, USA*

<sup>2</sup>*Department of Physics and Institute for Accelerator Science,  
Kangwon National University, Chuncheon 24341, Korea*

(Dated: January 6, 2022)

## I. CALCULATIONS OF STRUCTURAL PHASES IN FePS<sub>3</sub> UNDER PRESSURE

The layered material FePS<sub>3</sub> is composed of a 3-layer unit where a honeycomb lattice layer of Fe with a vertical P dimer at the Fe hexagon center lies in between two S triangular lattices. At ambient conditions, the 3-layer units are stacked in a staggered way with vdW gaps, adopting the monoclinic space group  $C2/m$  (#12) which we call HP0-SPD (staggered P dimers) phase. The material is reported to undergo two structural phase transitions under pressure [1]. The first phase transition involves inter-layer sliding (Fig. S1a, b) at  $\approx 4$  GPa, making the P dimers almost aligned but still preserving the monoclinic symmetry with the monoclinic angle slightly off  $90^\circ$ . This phase will be called HP1-APD (aligned P dimers). The second phase transition involves inter-layer collapse (Fig. S1b, c) at  $\approx 14$  GPa that gives rise to the formation of P chains (as opposed to separate P dimers) and changes the symmetry to  $P\bar{3}1m$  (#162). We call this phase HP2-APC (aligned P chain). The sliding transition is a necessary condition for the realization of HP2-APC since the linear alignment of the P dimers is a structural prerequisite for the formation of P chains that stabilize the collapsed phase HP2-APC. Our DFT calculations for enthalpy reproduce the two structural phase transitions (Fig. S2a, b) in agreement with the recent experimental and theoretical studies [1, 2]. Notable changes in the lattice constant  $c$  and the volume occur during the transition from HP1-APD to HP2-APC as expected from the formation of P chains (Fig. S2c, d). We also find that the structural phase transitions remain the same for the non-hydrostatic and the hydrostatic conditions.

As described in the main text, we relaxed the internal atomic coordinates using eDMFT while the lattice parameters (i.e., lattice constants and angles) were fixed to the values obtained by VASP since the stress is not available in eDMFT. The internal coordinates from eDMFT can be significantly different from those obtained by DFT due to the correlation effects. For example, eDMFT is more reliable than DFT in the calculation of the height of Se atoms in an iron-based superconductor FeSe [3]. In our system, we find that the difference in Fe-S bond lengths can be as large as  $\approx 1.8\%$  between eDMFT and DFT results.

## II. EFFECT OF HUND'S COUPLING IN HP1-APD

The realization of the OSMP in HP1-APD requires sizable strength of the Hund's coupling. If we artificially set  $J_H = 0$  in the calculation of HP1-APD, the OSMP does not appear (Fig. S3), and the PDOS becomes similar to that

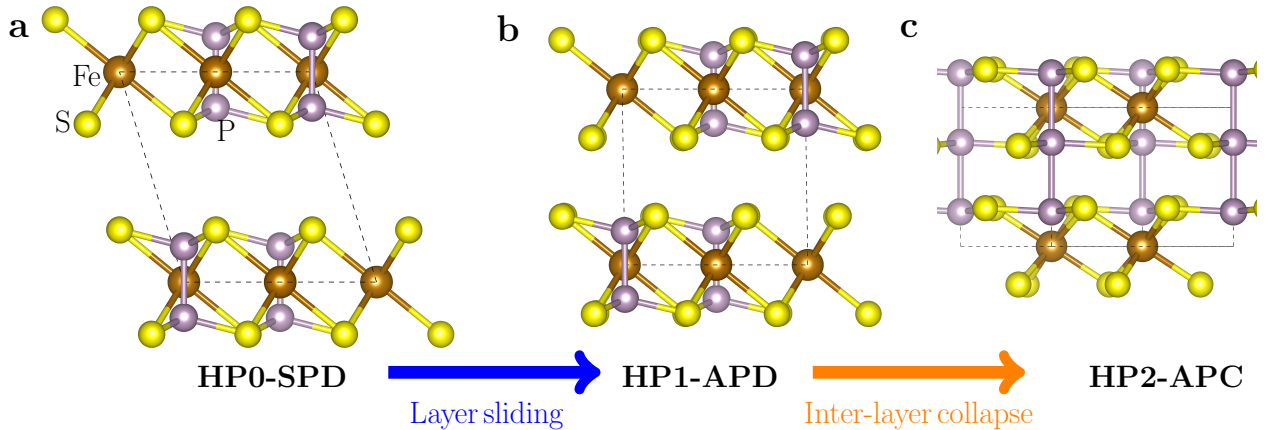


FIG. S1. Crystal structure of FePS<sub>3</sub>. Atomic structures of (a) HP0-SPD at 0 GPa, (b) HP1-APD at 10 GPa, and (c) HP2-APC at 18 GPa.

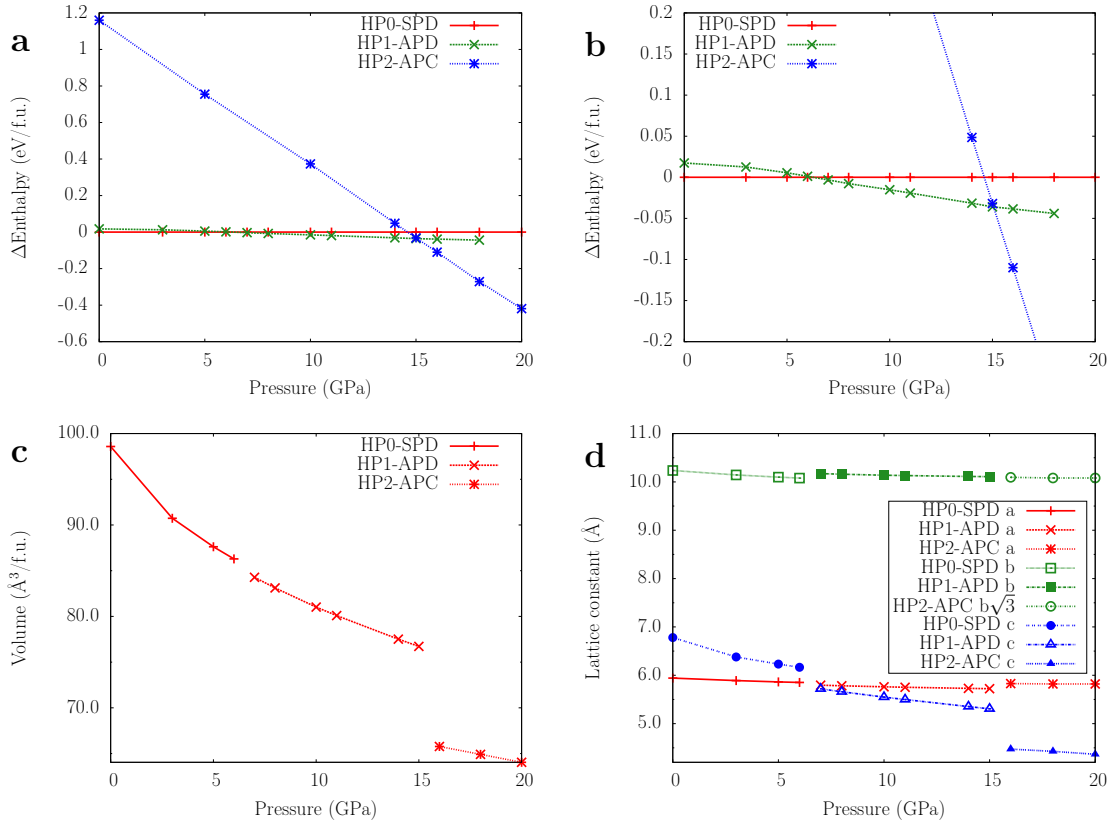


FIG. S2. Structural phase transitions in FePS<sub>3</sub>. (a) Relative enthalpy with respect to HP0-SPD, and a magnified view in (b). Evolution of (c) volumes and (d) lattice constants under pressure.

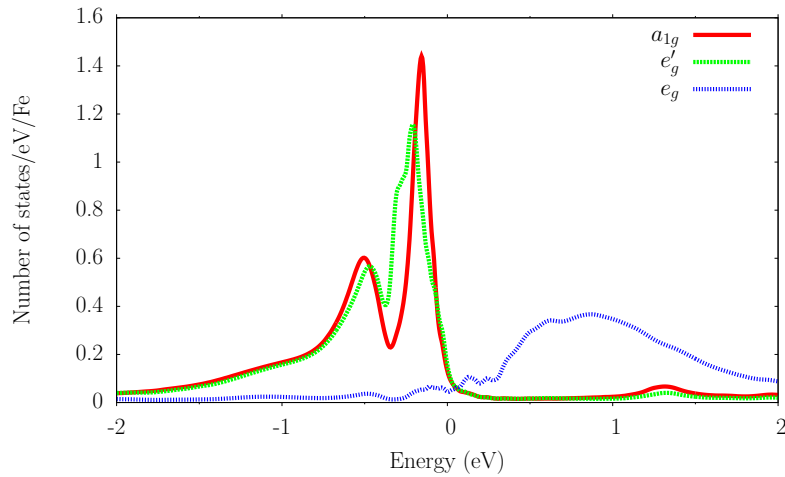


FIG. S3. PDOS of HP1-APD at 10 GPa with  $U = 8.0$  eV and  $J_H = 0.0$  eV.

32 of HP2-APC in which electrons mostly occupy  $t_{2g}$  states. The importance of the Hund's coupling in the realization  
 33 of the OSMP is in agreement with a theoretical report using three-band model Hamiltonian [4]. Thus, considerable  
 34 strength of the Hund's coupling (compared with the crystal-field splitting) is essential to realize the OSMP in FePS<sub>3</sub>.

### III. EFFECT OF ANISOTROPY IN PRESSURE

35

36 To understand the effect of anisotropy in pressure on the metallicity of HP1-APD, we calculate PDOS for different  
 37 values of  $P_r$  ( $= P_{zz}/P$ ) with  $P = \frac{P_{xx}+P_{yy}+P_{zz}}{3} = 10$  GPa. We find that larger out-of-plane component tends to favor  
 38 the metallic HP1-APD realizing the OSMP (Fig. S4). Also, under the hydrostatic pressure (i.e.,  $P_r = 1.0$ ), the system  
 39 has a small gap in agreement with the experiment [5]. We find that the anisotropy in pressure tends to increase the  
 40 hybridization in  $t_{2g}$  states, favoring the metallization (Fig. S5). This can be attributed to the fact that the larger  
 41 out-of-plane pressure component tends to reduce the Fe-S bond lengths in this layered structure.

42

### IV. EFFECT OF COULOMB INTERACTION

43 Experimentally, the HP1-APD phase is gapped under the hydrostatic pressure and becomes metallic under the non-  
 44 hydrostatic condition. In our calculations, we used  $U = 8.0$  eV and  $J_H = 0.8$  eV which give consistent results with the  
 45 experiments. Also, we tested the effect of smaller Coulomb parameter  $U$  in view of the metallicity of the HP1-APD  
 46 phase. We find that  $U = 7.0$  eV gives metallic PDOS for HP1-APD at 10 GPa (Fig. S6), which is inconsistent with  
 47 the experiments.

- 
- 48 [1] C. R. S. Haines, M. J. Coak, A. R. Wildes, G. I. Lampronti, C. Liu, P. Nahai-Williamson, H. Hamidov, D. Daisenberger,  
 49 and S. S. Saxena, Phys. Rev. Lett. **121**, 266801 (2018).  
 50 [2] Y. Zheng, X.-x. Jiang, X.-x. Xue, J. Dai, and Y. Feng, Phys. Rev. B **100**, 174102 (2019).  
 51 [3] K. Haule and G. L. Pascut, Phys. Rev. B **94**, 195146 (2016).  
 52 [4] L. de' Medici, S. R. Hassan, M. Capone, and X. Dai, Phys. Rev. Lett. **102**, 126401 (2009).  
 53 [5] M. J. Coak, D. M. Jarvis, H. Hamidov, C. R. S. Haines, P. L. Alireza, C. Liu, S. Son, I. Hwang, G. I. Lampronti,  
 54 D. Daisenberger, P. Nahai-Williamson, A. R. Wildes, S. S. Saxena, and J.-G. Park, Journal of Physics: Condensed Matter  
 55 **32**, 124003 (2019).

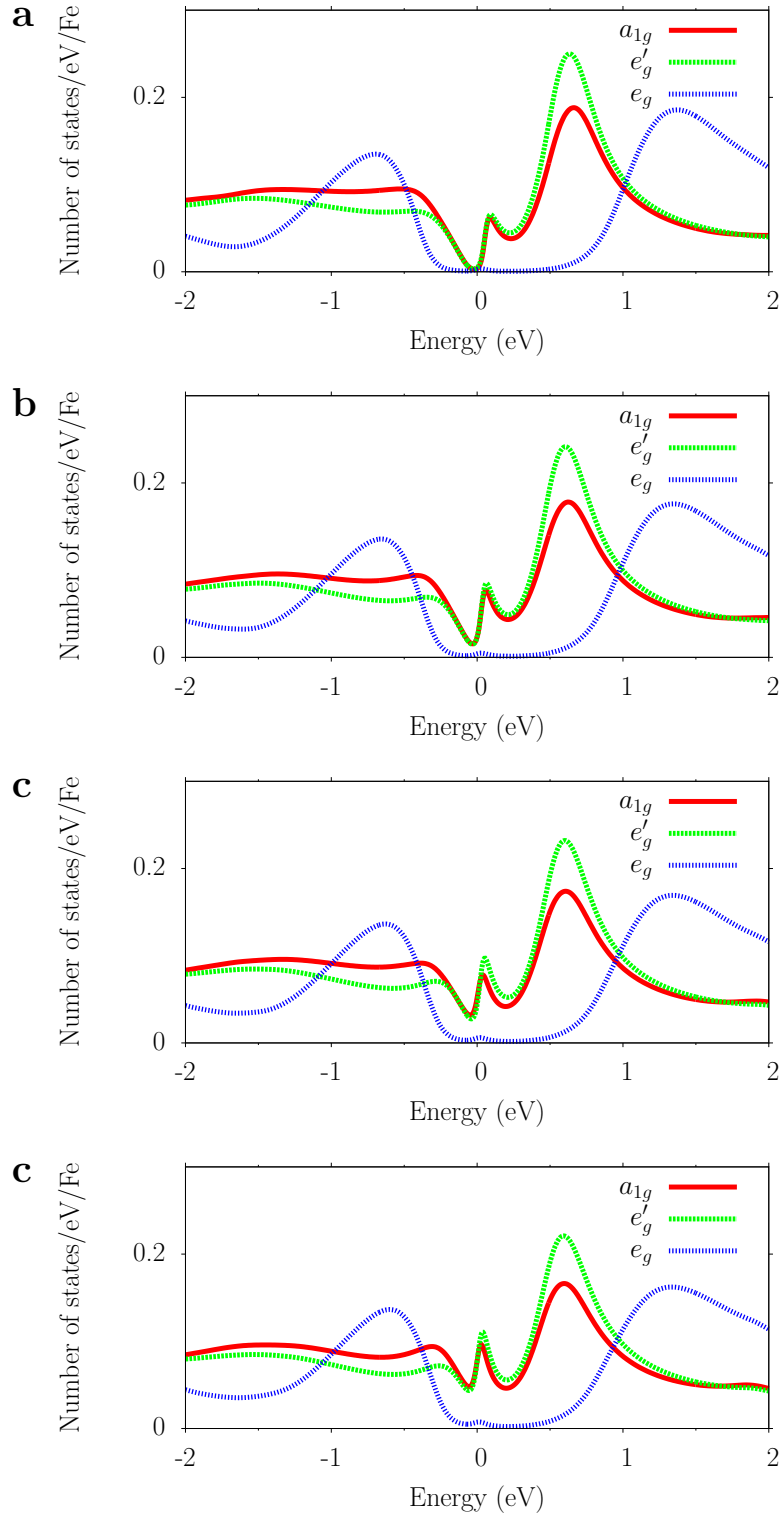


FIG. S4. PDOS of HP1-APD with different anisotropy in pressure at  $P = 10$  GPa. PDOS for (a)  $P_r = 1.0$ , (b)  $P_r = 1.2$ , (c)  $P_r = 1.3$ , and (d)  $P_r = 1.4$ .

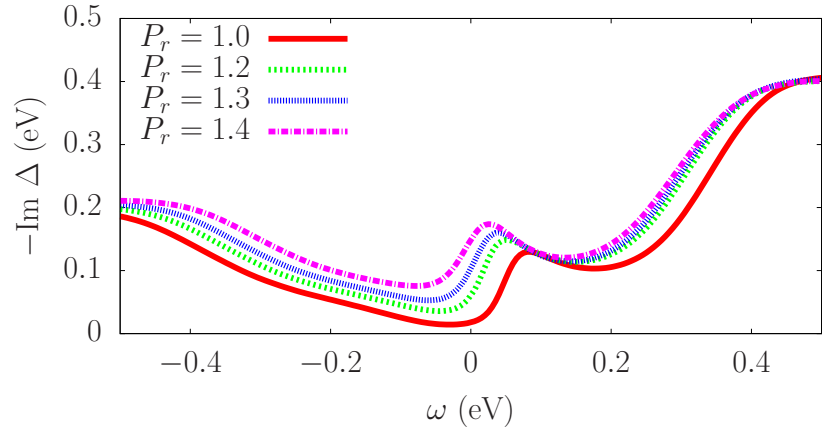


FIG. S5. Imaginary part of the impurity hybridization function  $\Delta$  in the  $a_{1g}$  state of HP1-APD with different anisotropy in pressure at  $P = 10$  GPa.

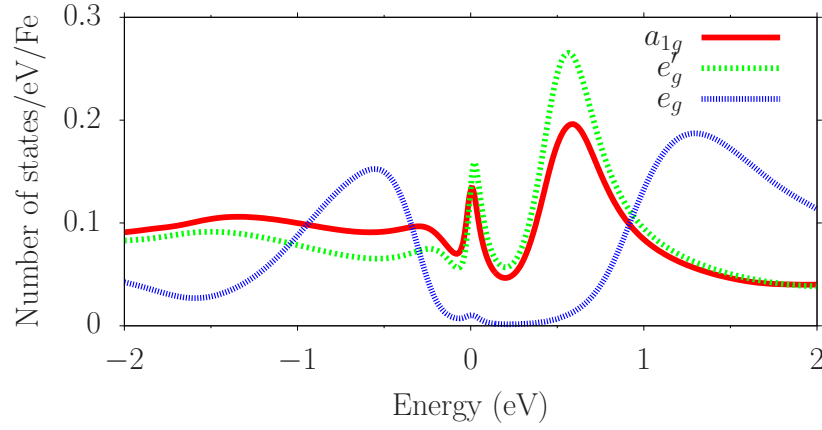


FIG. S6. PDOS of HP1-APD at 10 GPa under hydrostatic pressure with  $U = 7.0$  eV and  $J_H = 0.8$  eV.